

## Advanced Materials Methods Driving New Life in Critical Infrastructure

Guillermo A. Riveros

Information Technology Laboratory, US Army Engineer Research and Development Center, Vicksburg, MS 39180, ([Guillermo.A.Riveros@usace.army.mil](mailto:Guillermo.A.Riveros@usace.army.mil))

Hussam Mahmoud

Dept. of Civil and Environmental, Engineering, Colorado State Univ., Fort Collins, CO 80523, ([Hussam.Mahmoud@colostate.edu](mailto:Hussam.Mahmoud@colostate.edu))

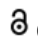
Emad M. Hassan


Dept. of Civil and Environmental, Engineering, Colorado State Univ., Fort Collins, CO 80523, ([Shafik@colostate.edu](mailto:Shafik@colostate.edu))

### Author Keywords

Experimental; Navigation Steel Structures, Steel panels; Retrofit; Basalt fibers

**Type:** Research Article

 Open Access

 Peer Reviewed

 CC BY



### Abstract

Fatigue damage is a major threat to many hydraulic steel structures (HSS). HSS experience fatigue loading during operation and are exposed to harsh environmental conditions that reduce fatigue life. The common methods to inspect and repair HSS is time-consuming and costly. Studies investigating the use of bonded Carbon and Basalt fiber reinforced polymer (CFRP, BFRP) to repair fatigue cracks in HSS are lacking. The main objectives of this study was to increase the bonding of FRP, investigate the effectiveness of different fiber-reinforced polymers, and perform experiments on different retrofitting configurations. In this study, eight large-scale center-cracked panels were tested under mode I loading under different environmental conditions, repair materials, and retrofitting configurations. Results indicated that the use of both CFRP and BFRP are both effective at extending fatigue life. Steel retrofitted with full patches of BFRP that cover the crack can reached infinite fatigue life. This article will conclude with several examples where FRP's have been used to repair lock gates.

## 1. Introduction

The United States inland waterways system has over 240 locks that form the Nation's "water highway" for freight transportation (Waterways Council, Inc. 2021). Freight moves via a system of towboats, which push barges lashed together as tows; each barge is capable of holding 1400–1800 tons of cargo. This complex infrastructure system, operated and maintained by the U.S. Army Corps of Engineers (USACE), delivers 4% by tonnage of US freight by waterway infrastructure (Waterways Council, Inc. 2021) and is the most economical transportation method (Port of Pittsburg Commission). This segment of the system provides an irreplaceable transportation resource that is essential for the carriage of the agricultural and industrial goods in the U.S. (Waterways Council, Inc. 2021, Waterways Council, EBP U.S. 2021).

In the last three decades, miter gates, (the most common lock gates) (Fig. 1) have experienced a significant amount of distress. Welded connections with low fatigue resistance, poor weld quality, unanticipated structural behavior, or unexpected loading due to the deterioration of the design boundary conditions are the causes of fatigue cracking. (Riveros and Arredondo 2011; Riveros et al. 2009; Mahmoud et al. 2014; Mahmoud and Riveros 2014, Riveros et al. 2022).

The main problem arise that the traditional methods to repair fatigue cracks on miter gates (Hole drilling, Vee-and-weld, Adding doubler/splice plates) that where mostly developed for pure tension cracks (Mode I) have proven ineffective, because miter gates experience tension/shear cracking (Mix-Mode) (Figure 1). While existing repair methods can provide solutions to continue safe operation, frequent inspection and repair are still required afterward. This is cumbersome and costly, as dewatering and inspection can require a structure to be temporarily taken out of service.

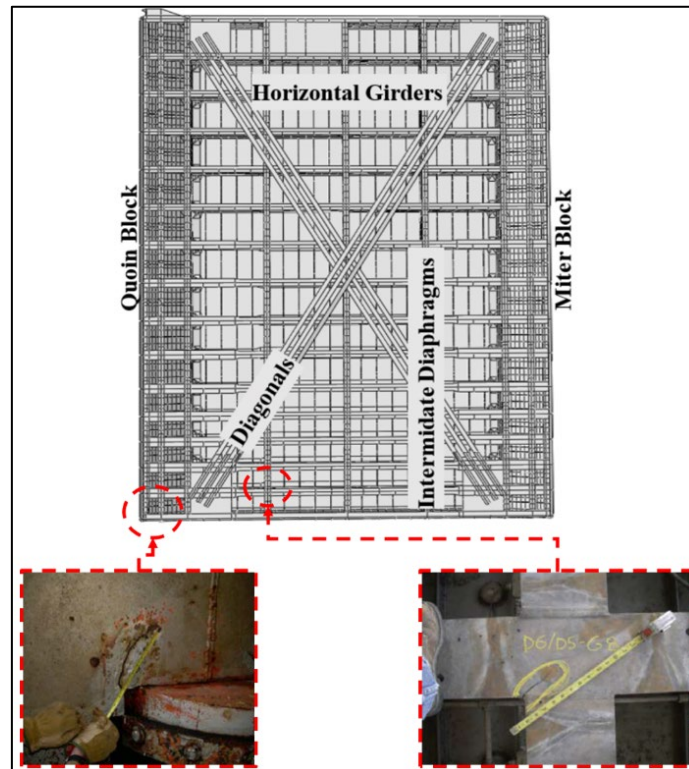


**Figure 1:** Examples of mixed mode cracks on a miter gate's pintle socket and front flange (Riveros and Lozano 2019).

Due to the challenges associated with implementing conventional repair methods in SHSs, alternatives that are simple to implement and reliable are of interest. Recent work has proposed that fiber-reinforced polymer (FRP) overlays offer a potential solution when used to repair cracks in SHS. FRPs have long since been used for general strengthening and repair of structural components, and as summarized by Mahmoud and Riveros (2013), they have been shown to be effective when used to reduce the rate of fatigue crack propagation in metallic structures. However, the applicability of FRP repairs for fatigue in underwater environments has not been fully explored, and their effectiveness was limited by poor adhesion to the steel substrate (Mahmoud et al. 2018). For instance, recent studies by Li et al. (2019, 2022) and Deng et al. (2022) concluded that the wetting and drying cycles using NaCl solutions can significantly reduce the fatigue resistance of interfacial debonding of steel beams strengthened by pre-stressed CFRP plate. Therefore, additional work is needed to maximize adhesion in an underwater environment to better increase the fatigue life of repaired cracks. Various studies have been carried out to assess the use of FRP for the rehabilitation of the increasingly aging and deteriorated civil structures and infrastructure systems in the United States. The deterioration is typically manifested in terms of fatigue cracking or corrosion cracking. Most previously conducted studies were aimed at investigating the use of FRP for

flexure and shear retrofitting of concrete structures (Maruyama 1997; Meier and Betti 1997; Neale and Labossiere 1997; Täljsten 1997; Thomas 1998; Triantafillou 1998; Miramiran et al. 2004). The studies highlighted the significant potential of such an application as demonstrated by the numerous field implementations of FRP repair of concrete structures. Much less research has been conducted on the use of FRP in strengthening metallic structures, with most studies geared toward flexure retrofitting of aluminum panels in the aviation industry (ASCE Committee on Composite Construction 2006). In general, research efforts on retrofitting steel elements have examined the repair of naturally deteriorated steel girders, repair of an artificially notched girder or steel plates to simulate fatigue cracks, strengthening an intact section to increase stiffness, and increasing the composite action between the steel girder and concrete deck in bridge application (Shaat et al. 2004).

## 2. Experimental Program

Constant amplitude Mode I fatigue experiments on eight unrepaired and repaired plates with dimensions of 1mx1m, a thickness of 9.5mm, and centered 102 mm precut crack (Figure 2) and different arrangements of Fiber Reinforced Polymers (FRP) were undertaken to determine the effectiveness of repairs perform with FRP. Specimens were submerged in fresh water to simulate the service environment experienced by HSS.

The first unretrofitted specimen (specimen S1) was tested in dry condition to create a reference point and determine the reduction in fatigue life caused by the underwater environment. Experiments on the second unretrofitted specimen (specimen S2) where conducted in freshwater to create a comparison against the repaired specimens and to simulate the environment experienced by HSS.

The repaired specimens used two layers of FRP on each face. CFRP was used for specimen 3 and 5. While Basalt fibers (BFRP) was used for and specimen 4 and 6. The retrofit method and test environment for each specimen are summarized in Table 1. Figure 3 shows dimension of the retrofitted specimens.

Specimen	FRP Type	FRP Layers	FRP configuration	Environment
S1	None	0	None	Air
S2	None	0	None	Fresh Water
S3	Carbon	2	Two patches	Fresh Water
S4	Basalt	2	Two patches	Fresh Water
S5	Carbon	2	Two patches	Fresh Water
S6	Basalt	2	Two patches	Fresh Water
S7	Carbon	2	Full patch	Fresh Water
S8	Basalt	2	Full patch	Fresh Water

**Table 1:** The test matrix as shown in Table 1

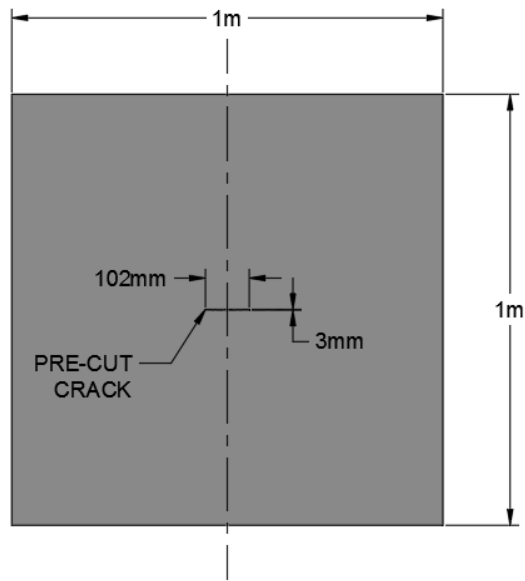


Figure 2: Dimensions of center-cracked steel plates

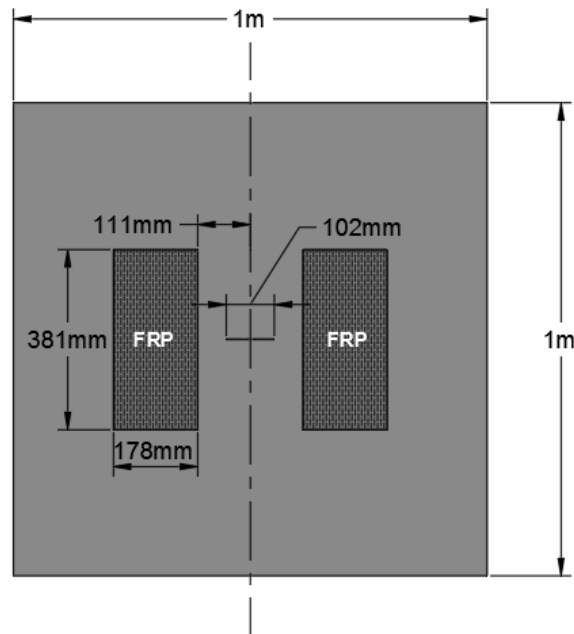
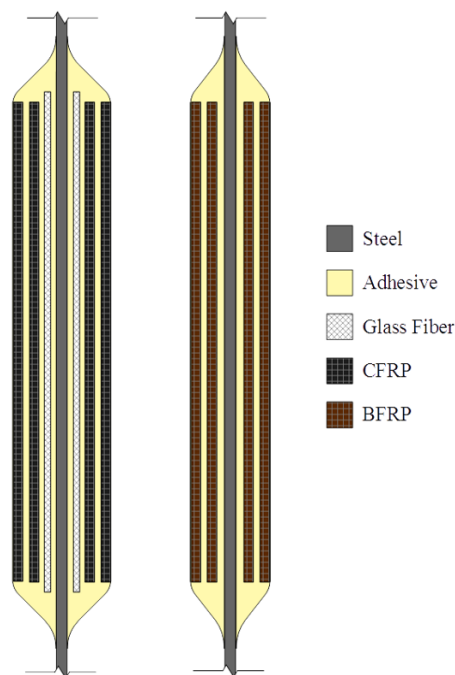


Figure 3: Dimensions of retrofitted specimens

An adhesive epoxy was used between the steel and FRP patch and between subsequent layers of FRP to improve bonding. A spew fillet was also formed from the adhesive around the perimeter of the FRP patch to reduce stress concentrations and prevent debonding at the patch ends. For the specimen repaired with CFRP, an additional layer of glass fiber fabric was installed between the steel and CFRP to provide an insulating barrier and prevent galvanic corrosion. Cross-sectional views of the FRP patch locations are illustrated in Figure 4.



**Figure 4:** Cross-sectional view of FRP patches

### 3. Material Properties

Both FRP systems were made from unidirectional fiber fabrics that were saturated with epoxy to form composites. The carbon fabric used was Tyfo SCH-41, manufactured by Fyfe Co. The basalt fibers are manufactured by Textum OPCO, LLC (Belmont, North Carolina). Tyfo S epoxy made by Fyfe Co. was used as the resin for both fiber types. Tyfo TC epoxy made by Fyfe Co. was used as the adhesive. The mechanical properties of materials are provided in Table 2. The plates used were structural rolled steel with 9.5 mm (3/8 in) thickness. A bi-directional glass fiber fabric was used for the insulation for the CFRP repaired specimen.

Material	Tensile Strength (MPa)	Tensile Modulus (GPa)
Steel	250	200
Carbon Fiber (Tyfo SCH-41)	4000	230
Basalt Fiber	1200-2200	65-90
Saturant Epoxy (Tyfo S)	72.4	3.18
Adhesive Epoxy (Tyfo TC)	22.7	1.2

**Table 2:** Material properties

Average thickness of the CFRP measured from coupons was approximately 2 mm. For the BFRP, average measured thickness from coupons was 3 mm. The CFRP and BFRP were not intended to have equivalent stiffness; although, the larger thickness of the BFRP can partially account for its reduced tensile modulus in comparison to the CFRP. Although adhesive application was not perfectly even, the average thickness of an adhesive layer was approximately 3 mm.

#### 4. Retrofit Application

The required carbon, glass, and basalt fiber fabrics were cut to size and wiped with a cloth dampened with acetone to remove any dust. Glass fibers were cut approximately 13 mm (1/2 in) larger in both dimensions than the carbon fibers to ensure an adequate insulating layer should there be any slight misalignment during application.

A wet layup process was used to apply the FRP patches. Proper adhesion and fiber alignment were critical during the application process because they are important for the performance of the retrofit. However, the installation process was not intended to be highly precise because it is ultimately intended to be feasible for applications in the field rather than a controlled laboratory environment.

FRP patches were applied one at a time. Adhesive was spread on the roughened steel surface in a uniform layer using a spatula. A layer of fibers was then placed on top of the adhesive and gently pressed into the adhesive and smoothed to remove any air bubbles and align fibers. Additional alternating layers of adhesive and fibers were applied as needed for each specimen. Before being placed, carbon fibers and basalt fibers were saturated with Tyfo-S. Fibers were fully submerged in the saturant and then removed and gently stripped of excess by hand. Placement was such that the unidirectional fibers were aligned perpendicular to the crack plane. The glass fiber fabric layers were not saturated. The FRP application process is illustrated in Figure 5.



Figure 5: FRP patch retrofit application process

##### 4.1. Experimental Test Set-Up

A self-reacting steel frame was designed to support the specimen and MTS hydraulic actuator and resist the cyclic load applied to the specimen. Conceptually, the test frame was identical to that used by Mahmoud et al. (2018), but beam and column sizes were increased to extend the frame's fatigue life.

An acrylic tank was built surrounding the specimens for use when an underwater test environment was needed. The steel tank floor rested on the lower test frame beam. A schematic of the test frame and water tank as viewed looking south is provided in Figure 6. A photo of the test system viewed looking south is shown in Figure 6.

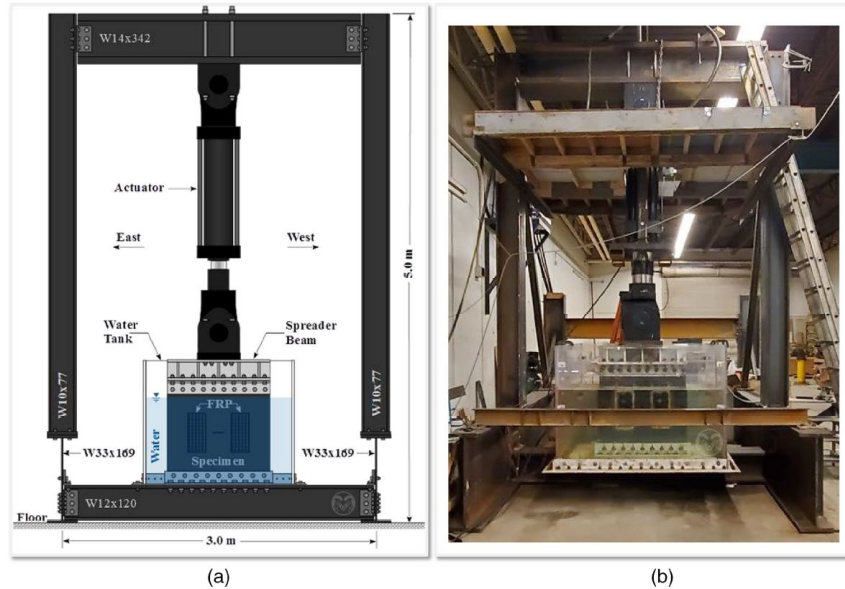


Figure 6: (a) Schematic of self-reacting test frame looking south; and (b) photo of the test frame.

#### 4.2. Strain Gauges

Strain gauges were installed on each specimen as shown in Figures 7. Specimen 1 included strain gauges located above the crack plane to verify the applied nominal stress. All specimens had multiple strain gauges installed along the crack plane. Readings from these gauges were expected to increase with crack growth and grow rapidly as the crack approached a gauge. For the retrofitted specimens, additional strain gauges were used to monitor FRP debonding, if any, by placing them along the height of the patches. A drop in a reading from a gauge on the FRP indicated that the bond directly beneath it was no longer intact. Strain gauges applied to specimens 2 through 8 were covered in silicone sealant to protect them from the water. A National Instruments PXI data acquisition system was used for recording strain readings.

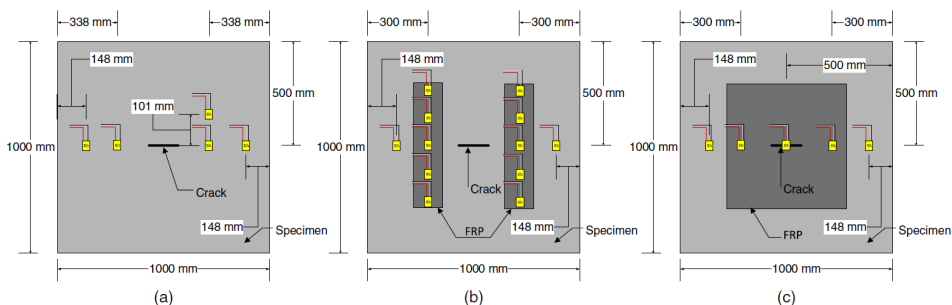


Figure 7: Strain gauge layout for: (a) specimen S1; (b) specimens S2 to S6; and (c) specimens S7 and S8.



### **4.3. Experimental Procedure**

Specimens were subjected to a constant stress range of 55 MPa and frequency of 0.6 Hz. A slightly positive stress ratio of 0.1 was selected to avoid reversing the load on the test frame. Load directives were sent to the actuator using an MTS FlexTest controller. Force and displacement responses were recorded by the controller. Strain data were logged continuously throughout the experiments using the data acquisition system.

At the start of each experiment, the initial crack was monitored closely to detect crack initiation. Crack elongation was taken to begin when a crack had initiated and grown through the tack welds. Crack length was then measured manually to the nearest 1.5 mm in regular increments for the experiment duration.

For the retrofitted specimens, crack lengths were only measured when the crack tip was not beneath an FRP patch since no additional method for detecting the crack through the FRP was implemented. Visual observations of retrofit behavior were also made throughout the experiment to identify any debonding for comparison to that detected by the strain gauges along the length of the FRP patches.

Experiments were considered complete when fracture of the specimen was imminent. Specimens were not intended to be tested to fracture due to the fracture could cause a possible misalignment or affecting bolt pretension. Typically, the crack grew to 100 mm to 120 mm away from the specimen edge before crack growth accelerated dramatically and the test was stopped.

### **4.4. Discussion of Results**

Crack progress versus the number of cycles and strain in the steel and FRP, were recorded throughout the experiments. Comparison of specimens S1 and S2 allowed for the harmful effect of the underwater environment to be quantified. The effectiveness of the retrofit methods was determined by comparison of the repaired specimens to the unrepaired specimens.

Comparison of specimens S3 and S5 with specimens S4 and S6 permitted the investigation of the use of BFRP as an alternative to CFRP. The influence of the patch shape was examined by relating the repaired specimens with two patches (specimens S2 to S6) with the repaired specimens with a full patch (specimens S7 and S8). During each experiment, crack extent was measured for the east and west cracks on both the north and south faces, and the average values for the east and west cracks were recorded each time that measurements were taken. The maximum strain values recorded during the time between the crack measurements are utilized to compare the strain data in this section. Observations of the crack behavior were made for each specimen during and after the tests.

In addition, the FRP bond was closely monitored for the retrofitted specimens. Debonding around the edges of the adhesive was detected. The failure mode of the FRP was observed at the end of tests of retrofitted specimens as either debonding failure, fiber rupture failure, or a combination. The galvanic corrosion was not directly measured during the test and the debonding around the edges was utilized as an indication of a possible galvanic effect. Details on the behavior of each specimen are noted in the following sections.

At the early stage of the tests prior to the cracks reaching the FRP patches, the growth rate of the cracks is lower for specimens retrofitted using CFRP as a result of the higher stiffness of the CFRP patches, promoting crack closure. However, as the crack continues to propagate, the high stiffness of the CFRP patches attracted larger forces, causing some debonding in the



patches. On the other hand, the BFRP has lower stiffness, causing it to be less effective in closing the crack in the early stages of the propagation. However, the lower stiffness characteristic is beneficial overall in reducing stresses in the repairs and eliminating debonding.

### 5. Fatigue Life

The fatigue life was used as the primary metric for comparing results across specimens and determining the effectiveness of the retrofits. As expected, all proposed retrofitting methods improved fatigue life, and the underwater environment reduced fatigue life in comparison to fatigue in air condition. Crack growth data for all specimens are shown in Figure 8. For all the specimens, the cracks initiated from the tack welds at both ends of the precut crack at approximately the same time. The initial phase of crack propagation is affected by the presence of the tack welds on both sides of the introduced crack. The number of cycles measured before the crack grew past the tack welds was 87,173, 80,000, 92,000, 94,000, 90,000, and 96,000 for specimens S1 to S6, respectively. However, no initiation was recorded for specimens S7 and S8. The cycles associated with initiation caused by the tack welds were subtracted from the total number of cycles reported for each test.

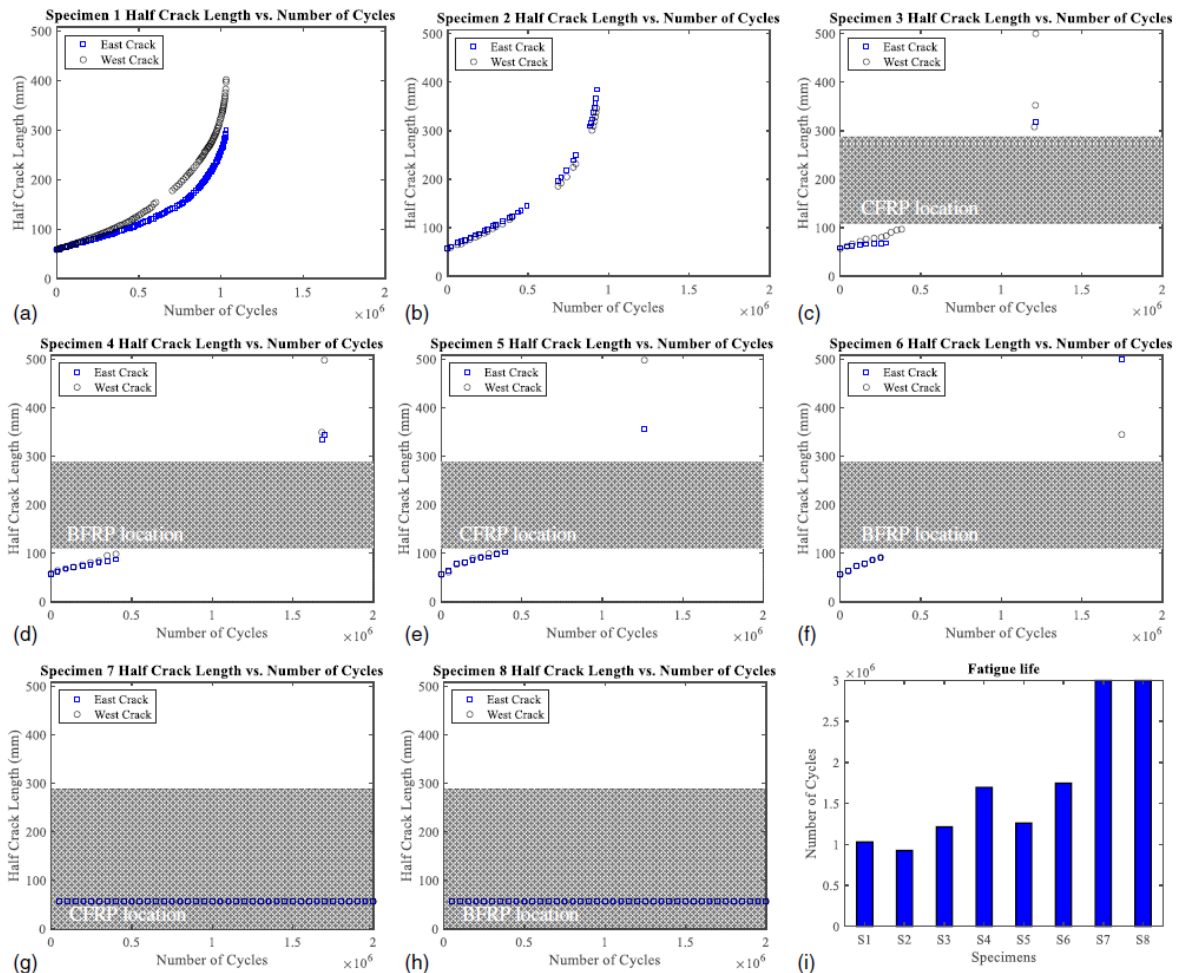


**Figure 8:** Crack propagation: (a) specimen 1; (b) specimen 2; (c) specimen 3; (d) specimen 4; (e) specimen 5; (f) specimen 6; (g) specimen 7; and (h) specimen 8 as well as (i) fatigue life comparison for all specimens.

Fig. 6(a) shows that for specimen S1, the two crack tips propagated at similar rates until reaching a half crack length of 75 mm. After this point, the west crack began to propagate more quickly than the east crack. The difference in length between the two cracks increased throughout the test; however, at the completion of the test, the west crack was 100 mm longer than the east crack. Measurements of crack growth for specimen S2 are shown in Fig. 6(b). The two crack tips propagated at similar rates until reaching a half crack length of 200 mm. After this point, the east crack began to propagate more quickly than the west crack. At the completion of the test, the east crack was 40 mm longer than the west crack. For specimen S3, the west side of the crack immediately began to grow more quickly than the east side as shown in Fig. 6(c). The width of the adhesive extending beyond the CFRP varied slightly at each location but was approximately 80 mm from the tack welds. The west crack reached a length of 93 mm at 380,000 cycles before reaching the adhesive. The east crack reached a length of 68 mm at 285,000 cycles and then could no longer be measured. Cracks in specimen S4 began to propagate on both sides of the initial notches at the same time. Crack propagation results are shown in Fig. 6(d). The width of the adhesive extending beyond the BFRP varied slightly at each location. The length of the west crack was 98 mm at 402,000 cycles before reaching the adhesive. The east crack reached a length of 87 mm at 402,000 cycles and then could no longer be measured. The two crack tips for specimen S5 almost propagated at similar rates until reaching the adhesive at 395,000 cycles, as displayed in Fig. 6(e). At the completion of the test, the west crack was 45 mm longer than the east crack. For specimen S6, the two crack tips propagated at similar rates until reaching the adhesive at 245,000 cycles, as shown in Fig. 6(f). At the completion of the test, the east crack was approximately 155 mm longer than the west crack. The cracks in specimens S7 and S8 did not propagate, as displayed in Figs. 6(g and h). A comparison between the fatigue life of all the tested specimens is shown in Fig. 6(i). A freshwater environment reduced the fatigue life by more than 10.3%. Utilizing two patches of CFRP can enhance the fatigue life between 31.1% and 36.3% compared with unretrofitted specimens tested in the underwater environment. However, using BFRP and the same repair configuration can improve the fatigue life between 83.4% and 89.0% compared with unretrofitted specimens tested in the underwater environment. Eventually, employing full patches that cover the crack resulted in infinite fatigue life for the specimens. These increases in the fatigue life were significant compared with a previous study by Mahmoud et al. (2018), where the fatigue life was only increased by 16% by using one layer of the CFRP sheet without an insulation layer of the glass fiber layer. The increase in performance in this study compared with the previous study (Mahmoud et al. 2018) is due to the effectiveness of the glass fiber in insulating the CFRP and preventing galvanic corrosion, the significance of using two layers of FRP in reducing the stresses on the crack plane, and efficiency of the BFRP in reducing the crack growth. To further reflect on the crack growth rate for the unrepaired specimens (in air and underwater), the parameters for the Paris Law were calculated from the test data. The Paris Law can be applied as a simple analytical method for understanding the growth rate of the test specimens' crack. Using the crack growth data acquired from specimens S1 and S2, the Paris Law parameters  $C$  and  $m$  were estimated by calculating crack growth rate ( $da/dN$ ) and stress intensity factor range ( $\Delta K$ ).  $C$  and  $m$  are the y-intercept and slope, respectively, of  $da/dN$  versus  $\Delta K$  plotted on a log-log scale, as shown in Fig. 7. Separate parameters were calculated for the east and west cracks. The difference between the estimated parameters for the east and the west cracks is minimal, which could be due to

uneven stress distribution in the specimen due to minute misalignment in the test setup. Calculated parameters are for crack length and stress intensity factor in units of mm and MPa $\sqrt{\text{mm}}$ , respectively. The first several crack length measurements were excluded from the calculation because they may have been affected by the presence of the tack welds. Additionally, measurements taken after unstable growth was noted were excluded, as the Paris Law no longer applies. A comparison between specimen S1, shown in Fig. 7(a), and specimen S2, displayed in Fig. 7(b), reveals that in each specimen, there was a difference between the crack growth rates for the east and west sides. The slope values for the east and west cracks,  $m$ , reduced from 2.51 and 1.58 for specimen S1 to 1.58 and 1.35 for specimen S2, reflecting the impact of the surrounding environment on the accelerating crack growth rates.

## Conclusions

This study focused on filling a significant gap in the literature pertaining to the effectiveness of basalt fibers in underwater fatigue repair of cracked steel panels. Eight large-scale CCT specimens were fabricated and tested under fatigue loading. Six of these specimens were retrofitted using bonded FRP patches and tested in an underwater environment and compared with unretrofitted specimens tested in an air and underwater environment. CFRP was used to retrofit three specimens, while the other specimens were retrofitted with BFRP. Special considerations were given to the quality of the bond between the steel and FRP. Two different configurations for the FRP patches were tested using either two separate patches or one full patch. A constant amplitude mode I fatigue test was carried out for each specimen. Crack growth and FRP behavior were monitored throughout the tests. Results from the different, retrofitted, and unretrofitted specimens were compared to identify the enhancement in fatigue life due to different environments, various FRP types, and a variety of FRP configurations. The following conclusions can be drawn from these tests:

- Results from the unretrofitted specimens tested in air and water confirmed the crack growth is accelerated underwater. Where a decrease in fatigue life of 10.3% was recorded when tested in an underwater environment. Although fatigue life was not reduced tremendously, the effect of the underwater environment can become substantial throughout the long service life.
- The retrofit methods using two patches of both CFRP and BFRP were shown to be viable for increasing fatigue life of a center-cracked panel with increases over the underwater unretrofitted specimen of 36.3% and 89.0% for CFRP and BFRP, respectively.
- CFRP performance was enhanced in this experiment testing compared with previously published studies as a result of using glass fiber as an insulating layer and proper application process, highlighting the need for the installation procedures when using the CFRP as a retrofit material in an underwater environment.

BFRP overperformed the CFRP due to its ability to avoid galvanic corrosion, enhance the durability in the underwater environment, and reduce the demand for the adhesive. Even though the sample size was small, the positive results of the BFRP specimens were promising that the BFRP can be the future repair of fatigue damage in steel, especially in an underwater environment.

- The higher stiffness of the CFRP was apparent when comparing crack growth and strain distribution with BFRP before the cracks reached the FRP patches. BFRP was also effective in the redistribution of the stresses over the tested specimens' components.
- The retrofitting configuration utilized has a significant impact on the expected fatigue life of the center-cracked panels. The results showed that using a single patch that covers the center

crack can assure an infinite fatigue life of the tested specimen. It can also significantly reduce the stresses on the crack tip and delay the crack opening.

- The results show that the use of glass fiber as an insulation layer between the CFRP and the steel and the use of BFRP to repair the steel structures subjected to high-cycle fatigue and submerged in the freshwater environment can significantly enhance fatigue life. While these findings are applicable to underwater cracked steel elements subjected to mode I fatigue loading and fabricated using different structural steel grades (AISC 2016), the impact of the element's exposure time to the harsh surrounding environment on the repair effectiveness needs further investigation.

## References

- Deng, J., J. Li, and M. Zhu. 2022. "Fatigue Behavior of Notched Steel Beams Strengthened by a Prestressed CFRP Plate Subjected to Wetting/Drying Cycles." *Composites, Part B* 230 (July): 109491. <https://doi.org/10.1016/j.compositesb.2021.109491>.
- EBP U.S., and ASCE. 2021. *Failure to Act: Ports and Inland Waterways—Anchoring the U.S. Economy*. Reston, VA: ASCE.
- Li, J., J. Deng, Y. Wang, J. Guan, and H. Zheng. 2019. "Experimental Study of Notched Steel Beams Strengthened with a CFRP Plate Subjected to Overloading Fatigue and Wetting/Drying Cycles." *Composite Structures* 209 (February): 634–43. <https://doi.org/10.1016/j.compstruct.2018.11.020>.
- Li, J., M. Zhu, and J. Deng. 2022. "Flexural Behaviour of Notched Steel Beams Strengthened with a Prestressed CFRP Plate Subjected to Fatigue Damage and Wetting/Drying Cycles." *Engineering Structures* 250 (October): 113430. <https://doi.org/10.1016/j.engstruct.2021.113430>.
- Mahmoud, H. N., and G. A. Riveros. 2013. *Fatigue Repair of Steel Hydraulic Structures (SHS) Using Carbon Fiber Reinforced Polymers (CFRP): Feasibility Study*. Vicksburg, MS: US Army Engineer Research and Development Center.
- Mahmoud, H. N., G. A. Riveros, M. Memari, A. Valsangkar, and B. Ahmadi. 2018. "Underwater Large-Scale Experimental Fatigue Assessment of CFRP-Retrofitted Steel Panels." *Journal of Structural Engineering* 144 (10): 04018183. [https://doi.org/10.1061/\(ASCE\)ST.1943-541X.0002184](https://doi.org/10.1061/(ASCE)ST.1943-541X.0002184).
- Mahmoud, H., A. Como, and G. A. Riveros. 2014. "Fatigue Assessment of Underwater CFRP-Repaired Steel Panels Using Finite Element Analysis." *ERDC/ITL TR-14-3*. Vicksburg, MS: U.S. Army Engineer Research and Development Center.
- Mahmoud, H., and G. A. Riveros. 2014. "Fatigue Reliability of a Single Stiffened Ship Hull Panel." *Engineering Structures* 66: 89–99.
- Maruyama, K. 1997. "JCI Activities on Continuous Fibre Reinforced Concrete, Non-Metallic (FRP) Reinforcement for Concrete Structures." *Japan Concrete Institute* 3–12.
- Meier, U., and R. Betti, eds. 1997. *Recent Advances in Bridge Engineering – Advanced Rehabilitation*. EMPA Switzerland: Durable Materials. Non-Destructive Evaluation and Management.
- Miramiran, A., M. Shahawy, A. Nanni, and V. Karbhari. 2004. *Bonded Repair and Retrofit of Concrete Structures Using FRP Composites - Recommended Construction Specifications and Process Control Manual*. NCHRP Report 514.

- Neale, K. W., and P. Labossière. 1997. "State-of-the-Art Report on Retrofitting and Strengthening by Continuous Fibre in Canada." *Non-Metallic (FRP) Reinforcement for Concrete Structures*. Japan Concrete Institute, 25–39.
- Riveros, G. A., F. J. Acosta, C. M. Lozano, and E. Glynn. 2022. "The Effects of Deteriorated Boundary Conditions on Horizontally Framed Miter Gates." *Metals* 12: 37. <https://doi.org/10.3390/met12010037>.
- Riveros, G. A., and E. Arredondo. 2011. "Predicting Deterioration of Navigation Steel Structures with Markov Chain and Latin Hypercube Simulation." *Revista Internacional de Desastres Naturales, Accidentes e Infraestructura Civil* 11 (1): 3–15.
- Riveros, G. A., J. L. Ayala-Burgos, and J. Perez. 2009. "Numerical Investigation of Miter Gates." *ERDC/ITL TR-09-1*. Vicksburg, MS: U.S. Army Engineer Research and Development Center.
- Riveros, G. A., and C. M. Lozano. 2019. "Blind Prediction of FRP Repairs for Multiaxial Fatigue Cracks on Hydraulic Steel Structures." *ICMFF 12*. Bordeaux: ICMFF.
- Täljsten, B. 1997. "Strengthening of Beams by Plate Bonding." *Journal of Materials in Civil Engineering* 206–12.
- Thomas, J. 1998. "FRP Strengthening – Experimental or Mainstream Technology." *Concrete International*, American Concrete Institute, 57–58.
- Triantafillou, T. C. 1998. "Shear Strengthening of Reinforced Concrete Beams Using Epoxy-Bonded FRP Composites." *ACI Structural Journal* 95 (2): 107–15.
- Waterways Council. 2021. *2021 Infrastructure Report Card: Inland Waterways*. Reston, VA: ASCE.
- Waterways Council. n.d. "Waterways System: Learn About the Future of Our Waterways." Accessed November 3, 2021. <https://www.waterwayscouncil.org/waterways-system>.
- Port of Pittsburgh Commission. n.d. "The Port District." Accessed November 3, 2021. <https://www.portpitt.com/pages/the-port-district>.

### **Acknowledgments**

The authors acknowledge the financial support provided by the U.S. Army Engineer Research and Development Center, Navigations System Research Program. Permission was granted by the Director of the Information Technology Laboratory to publish this information.